Smart Sensors, Measurement and Instrumentation 23

Subhas Chandra Mukhopadhyay
Octavian Adrian Postolache
Krishanthi P. Jayasundera
Akshya K. Swain *Editors*

Sensors for Everyday Life

Environmental and Food Engineering

Springer

Smart Sensors, Measurement and Instrumentation

Volume 23

Series editor

Subhas Chandra Mukhopadhyay
Department of Engineering, Faculty of Science and Engineering
Macquarie University
Sydney, NSW
Australia
e-mail: S.C.Mukhopadhyay@massey.ac.nz

More information about this series at http://www.springer.com/series/10617

Subhas Chandra Mukhopadhyay
Octavian Adrian Postolache
Krishanthi P. Jayasundera
Akshya K. Swain
Editors

Sensors for Everyday Life

Environmental and Food Engineering

Springer

Editors
Subhas Chandra Mukhopadhyay
Department of Engineering, Faculty of Science and Engineering
Macquarie University
Sydney, NSW
Australia

Octavian Adrian Postolache
Instituto de Telecomunicações
Lisbon
Portugal

and

ISCTE-IUL
Lisbon
Portugal

Krishanthi P. Jayasundera
Institute of Fundamental Sciences
Massey University
Palmerston North
New Zealand

Akshya K. Swain
Department of Electrical and Computer Engineering
University of Auckland
Auckland
New Zealand

ISSN 2194-8402 ISSN 2194-8410 (electronic)
Smart Sensors, Measurement and Instrumentation
ISBN 978-3-319-47321-5 ISBN 978-3-319-47322-2 (eBook)
DOI 10.1007/978-3-319-47322-2

Library of Congress Control Number: 2016953322

Printed on acid-free paper

This Springer imprint is published by Springer Nature
The registered company is Springer International Publishing AG
The registered company address is: Gewerbestrasse 11, 6330 Cham, Switzerland

Preface

Sensors play a pivotal role in our everyday life. They gather data on environment, and information on weather, traffic congestion, air pollution, water pollution, etc. is obtained; they gather data on human body, and information on health, treatment or therapy outcomes is obtained; they gather data on objects, and information for monitoring and control of these objects is obtained; they gather data on subjects or objects functions, and information for better decisions, control and action is obtained. For instance, the weather information is used to choose adequate clothes, the battery level sensor permits smartphone power management optimization, and the level of blood glucose allows better healthcare management. Data collected through sensors enhance our lives and our connections to each other and with our environment, allow real-time monitoring of many phenomena around us, provide information about quality of products and services, improve the equipment control based on sensorized interfaces and contribute to increase knowledge on physical and chemical world.

The advances in electronics, embedded controller, technology for communication as well as the progress towards a better informed, knowledge based society increase the demand for small size, affordable sensors that allow accurate and reliable data recording, processing, storing and communication. The work contains invited chapters from renowned experts, working in sensors' field, and it is split into two books that present several technologies and applications of sensors in *Environmental and Food Engineering* (ISBN 978-3-319-47322-2) and for *Healthcare Settings* (ISBN 978-3-319-47319-2).

The book *Sensors for Everyday Life—Environmental and Food Engineering* describes novel sensors and sensing systems developed for environment monitoring and food production and quality assessment.

Environmental quality refers to characteristics from natural environment as well as from the built environment (i.e. city air and/or water pollution, concentration of nitrate from the soil in cultivated fields). Environmental quality plays an important role in health and well-being of the populations. Degraded environmental quality as produced by air and water pollution may affect our lives, directly or through the food we eat. In food engineering various sensors are used for assessment of

contaminants, adulterants, naturally occurring toxins or any other substance that may make food injurious to health on an acute or chronic basis as well as sensors that contribute for quality improvement of food. New developed sensors and technology trend related air, water, food quality monitoring as well as for modern agronomy and food production are presented in this book.

How This Book is Organized

In Chap. 1, a novel method for the simultaneous determination of NOx and soot in the exhaust of diesel engines during the periodical technical inspection roadworthiness test is presented. A multi-wavelength light extinction measurement, in a setup similar to an opacimeter with high sensitivity, and a mathematical inversion algorithm are used to obtain the concentrations from the extinction readings.

Analytical technique of the fine particles using atomic emission spectroscopy system for an environmental pollution monitoring is presented in Chap. 2. Laser-induced breakdown spectroscopy (LIBS) system and the helium-microwave-induced plasma-atomic emission spectroscopy (He-MIP-AES) system are used for characterizations and real-time measurement of the air chemical compositions and particle size.

Chapter 3 presents sensors and method for automatic fault detection in heating ventilating and air conditioning (HVAC) systems. This is important mainly in smart buildings context as the indoor condition in these buildings is mainly related with the capabilities and reliability of HVAC systems.

New optical fiber humidity sensor is described in Chap. 4. Different humidity sensors that have been developed by now are presented focusing in the different optical structures and materials that have been used for improving sensitivity and resolutions of these sensors.

The measurement of air gas concentration represents an important field of application of sensing technologies. In Chap. 5 of the book, a review on the oxygen gas sensing technologies is presented with focus on potentiometric, amperometric, paramagnetic and tunable diode laser spectroscopy (TDLS) sensors. Theoretical aspects and operational basic of these technologies, system requirements as well as limitations of the methods are discussed in this chapter.

A low-cost sensor node based on interdigital capacitive sensor for nitrate and nitrite in surface and ground water concentration detection is presented in Chap. 6. This sensor is important for agronomy as well as for water pollution assessment. Nitrates may be present in high concentration in ground and surface water as a result of intensive agriculture, disposal of human and animal sewage and industrial wastes.

In Chap. 7 an intelligent wireless sensor network system designed to monitor various parameter in palm oil plantation for improvement in the controlled pollination process is presented. The system helps in making decision related to best time for pollination process. The inaccuracy in determining pollination readiness

of the oil palm flower could potentially cause a detrimental effect on the palm oil industry in the long run.

The following two chapters present sensors for determination of quality and quantity of water for drinking purpose. In Chap. 8, a reflectometer and a Doppler radar systems for detection of water level in septic tank is described. A novel S3 (Small Sensor System) nanowire device for the detection of complex mixtures of bacteria in potable water is presented in Chap. 9.

Next three chapters describe sensors used in food productions and quality assessment. A novel approach to monitor the quality of milk products, based on electromagnetic wave spectroscopy is presented in Chap. 10. The system use vector network analyser to capture spectral signatures in the form of scattering parameters from electromagnetic wave sensors. Data on reliability testing is presented. A new, rapid, portable, easy-to-use, economic and non-destructive fouling based on nanowire technology device to control the presence of false grated Parmigiano Reggiano cheese is described in Chap. 11. A review on the conventional techniques and dielectric spectroscopy for analyzing food products is presented in Chap. 12, focusing on the application of dielectric spectroscopy in fats and oils adulteration detection.

Different wireless sensor network architecture is implemented nowadays to perform distributed measurement tasks for environment monitoring with increase in space resolution. Big challenge in these implementations continues to be wireless interference and radio-frequency (RF) spectrum crowding. Chapter 13 focuses on a technique for optical-based RF interference cancellation. In this chapter several system architectures are presented and a sample of their experimental performance and the key characteristics of this technique and the future prospects for this technology, focusing specifically on photonic integrated circuits are discussed. A scheme is proposed in Chap. 14 that can reduce the performance difference between cluster heads (CHs) involved in inter-cluster communication on IEEE 802. 15.4 cluster-based wireless sensor networks (WSNs) under spatial non-uniform traffic condition where the CHs have various amount of traffic. This reduced the energy consumption and simplified processing mechanism to achieve long WSNs lifetime under limited network resource condition.

We do sincerely hope that the readers will find this special issue interesting and useful in their research on sensors and wireless sensor networks for environment monitoring, food production and quality assessment.

We want to acknowledge all the authors for their contribution and for sharing of their knowledge. We hope that the works presented in this book will stimulate further research related to sensors for everyday life.

Sydney, Australia — Subhas Chandra Mukhopadhyay
Lisbon, Portugal — Octavian Adrian Postolache
Palmerston North, New Zealand — Krishanthi P. Jayasundera
Auckland, New Zealand — Akshya K. Swain

About the Editors

Dr. Subhas Chandra Mukhopadhyay (M'97, SM'02, F'11) graduated from the Department of Electrical Engineering, Jadavpur University, Calcutta, India with a **Gold medal** and received the Master of Electrical Engineering degree from Indian Institute of Science, Bangalore, India. He has Ph.D. (Eng.) degree from Jadavpur University, India and Doctor of Engineering degree from Kanazawa University, Japan.

Currently he is working as Professor of Mechanical/Electronics Engineering and Discipline Leader of the Mechatronics Degree Programme of the Department of Engineering, Macquarie University, Sydney, Australia. He has over 26 years of teaching and research experiences.

His fields of interest include smart sensors and sensing technology, wireless sensor networks, internet of things, electromagnetics, control engineering, magnetic bearing, fault current limiter, electrical machines and numerical field calculation.

He has authored/co-authored over **400** papers in different international journals, conferences and book chapter. He has edited **thirteen** conference proceedings. He has also edited **fifteen** special issues of international journals as lead guest editor and **twenty-five** books with Springer-Verlag.

He was awarded numerous awards throughout his career and attracted over NZ $4.2 M on different research projects.

He has delivered **272** seminars including keynote, tutorial, invited and special seminars.

He is a **Fellow** of IEEE (USA), a **Fellow** of IET (UK) and a Fellow of IETE (India). He is a Topical Editor of IEEE Sensors Journal and an Associate Editor IEEE Transactions on Instrumentation. He has organized many international conferences either as general chair or technical programme chair. He is the

Ex-**Chair** of the IEEE Instrumentation and Measurement Society New Zealand Chapter. He chairs the IEEE IMS Technical Committee 18 on Environmental Measurements.

Dr. Octavian Adrian Postolache (M'99, SM'2006) graduated in Electrical Engineering at the Gh. Asachi Technical University of Iasi, Romania, in 1992 and he received the Ph.D. degree in 1999 from the same university, and university habilitation in 2016 from Instituto Superior Tecnico, Universidade de Lisboa, Portugal. In 2000 he became principal researcher of Instituto de Telecomunicações where he is now Senior Researcher. Since 2012 he joined Instituto Universitario de Lisboa/ISCTE-IUL Lisbon where he is currently Aux. Professor.

His fields of interests include smart sensors for biomedical and environmental applications, pervasive sensing and computing, wireless sensor networks, signal processing with application in biomedical and telecommunications, non-destructive testing and diagnosis based on eddy currents smart sensors, computational intelligence with application in automated measurement systems.

He is active member of national and international research teams involved in Portuguese and EU and International projects. He was principal researcher of different projects including EHR-Physio regarding the implementation of Electronic Health Records for Physiotherapy and he is currently principal researcher of TailorPhy project Smart Sensors and Tailored Environments for Physiotherapy.

Dr. Postolache is author and co-author of 9 patents, 4 books, 16 book chapters, 66 papers in international journals with peer review, more than 220 papers in proceedings of international conferences.

He is IEEE Senior Member I&M Society, Distinguished Lecturer of IEEE IMS, chair of IEEEI&MSTC-13 Wireless and Telecomunications in Measurements, member of IEEEI&MSTC-17, IEEEI&MSTC-18, IEEEI&MSTC-25, IEEE EMBS Portugal Chapter and chair of IEEE IMS Portugal Chapter. He is Associate Editor of IEEE Sensors Journal, and IEEE Transaction on Instrumentation and Measurements, he was general chair of IEEE MeMeA 2014, and TPC chair of ICST 2014, Liverpool and ICST 2015 in Auckland. He received IEEE best reviewer and the best associate editor in 2011 and 2013 and other awards related to his research activity in the field of smart sensing.

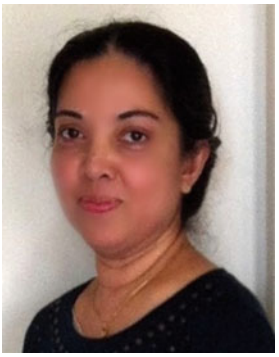

Dr. Krishanthi P. Jayasundera graduated from University of Peradeniya, Sri Lanka with honors degree in Chemistry. She obtained her both Master and Ph.D. in Organic Chemistry from Kanazawa University, Japan. She worked as postdoctoral researcher at Massey University nearly 14 years in New Zealand involving various projects focused on the chemical synthesis of architecturally interesting molecules which have biological, environmental and/or medicinal significance. Currently, she is an independent research consultant. She specializes in organic chemistry, biosciences, sensitivity analysis using NMR, HPLC, SPR and so on. She has published over 30 papers in different international journals and conference proceedings.

Akshya K. Swain received the B.Sc. degree in Electrical Engineering and the M.Sc. degree in Electronic Systems and Communication from Sambalpur University, Sambalpur, India, in 1985 and 1988, respectively, and the Ph.D. degree from the Department of Automatic Control and Systems Engineering, University of Sheffield, Sheffield, U.K., in 1997. From 1994 to 1996, he was a Commonwealth Scholar in the United Kingdom. Since September 2002, he has been with the Department of Electrical and Computer Engineering, the University of Auckland, Auckland, New Zealand. He has published over 150 papers in International Journals and conferences. His current research interests include nonlinear system identification and control, fault tolerant control, biomedical signal processing, sensor networks, and control applications to power system and wireless power transfer system. Dr. Swain is an Associate Editor of IEEE Sensors Journal and Member of the Editorial Board of International Journal of Automation and Control and International Journal of Sensors, Wireless Communications and Control.

Contents

Determination of NO_X and Soot Concentrations Using a Multi-wavelength Opacimeter

H. Axmann, A. Bergmann and B. Eichberger

Abstract A novel approach to measure both the particle and the NO_2 concentration in the exhaust of diesel engines during the roadworthiness test in the periodical technical inspection is presented. It is based on a multi-wavelength extinction measurement and a mathematical inversion algorithm to obtain the concentrations from the extinction readings. Such individual concentration values can deliver valuable insight into the cause of engine or exhaust aftertreatment defects. Furthermore the extended opacimeter provides future-proofness, if nitrous gas emissions are incorporated in the roadworthiness regulations. In addition to a detailed description of the multi-wavelength approach this chapter provides an overview of particle and nitrous gas emissions by diesel engines, the related legislation, the extinction measurement using standard opacimeters, and the physical background for this optical measurement method. The applicability of the multi-wavelength method is derived mathematically and validated with first experimental results as well as with simulations.

1 Introduction

The emissions of vehicles equipped with internal combustion engines pose a significant environmental problem and cause severe health effects. A big portion of the engines run on diesel fuel. In some European countries they even surpass the amount of gasoline vehicles with a relation of 70 to 30 % [1]. Across Europe the average fraction of newly registered diesel cars reached 58 % in 2011 [2]. While the main pollutant in the exhaust of gasoline engines is carbon dioxide (CO_2), the most

H. Axmann (✉)
AVL DiTEST GmbH, Alte Poststraße 156, 8020 Graz, Austria
e-mail: harald.axmann@avl.com

A. Bergmann · B. Eichberger
Institute of Electronic Sensor Systems, University of Technology,
Inffeldgasse 10/II, 8010 Graz, Austria

S. Mukhopadhyay et al. (eds.), *Sensors for Everyday Life*, Smart Sensors,
Measurement and Instrumentation 23, DOI 10.1007/978-3-319-47322-2_1

relevant pollutants of diesel engines are particulate matter (PM) and nitrous gases (NO_X). CO_2 is a green house gas, whereas particles and NO_2 are toxic components.

Diesel particulate matter consists mainly of carbonaceous particles, ashes and unburned fuel and oil droplets [3]. It has been lately proven to be carcinogenic [4]. Furthermore the black carbon (BC) fraction of the particles contributes to global warming, and when deposited on snowpacks the particles lead to accelerated melting through absorption of the sunlight [5].

Nitrous gases consist of nitrogen monoxide (NO) and nitrogen dioxide (NO_2). During the combustion process of diesel fuel mostly NO is produced. By the catalyzed particle filter systems in modern vehicles a significant amount of NO is oxidized to NO_2 [6–8]. NO_2 is a brown, toxic gas, which may lead to mucosal irritation. It is a main contributor to smog in big cities [9] and is—in aqueous solution—a strong acid leading to acid rain [10].

Governments all over the world reacted to this threat by introducing limits for the allowed concentration of said pollutants in the exhaust of internal combustion engines. Since the first emission regulations in the early 1970s the limit values have been significantly reduced [10–12]. This is shown in Fig. 1 using the European Emission Standards (EURO 1-6) as an example. To conform to these emission limits the engine manufacturers have to optimize the combustion process and to add new exhaust aftertreatment systems. Still the efficiency of these measures can deteriorate over time. Accordingly periodic emission checks are necessary to ensure the compliance of the vehicles to the emission limits. Such emission checks are typically performed during the periodical technical inspection (PTI) in garages or vehicle inspection institutions.

For the case of diesel vehicles the regulation-compliant functionality of the engine and the exhaust system is determined from the opacity of the exhaust gases. The corresponding measurement device is the opacity meter, commonly just called opacimeter, which is based on an optical measurement. Just as the first emission

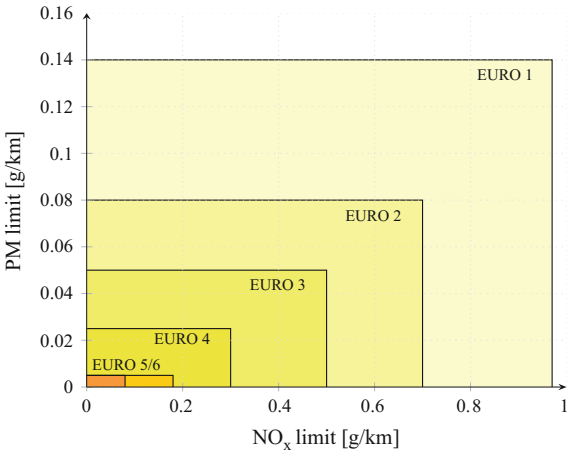

Fig. 1 PM and NO_X limits of EURO 1-6

limits its measurement principle dates back to the 1970s [13]: A measurement chamber of defined length is filled with exhaust gas, and the attenuation of light by the sample is measured. While this was working perfectly for the older diesel vehicles emitting tight black clouds of soot, it is reaching its limits for modern models [14]. Equipped with diesel particle filters (DPFs) they emit much less, very small particles. Accordingly the exhaust plumes are effectively transparent, only with a very small amount of opacity. Therefore updated or new measurement technologies are needed in order to perform meaningful and reliable measurements.

An example for a new technology is light scattering. It is also an optical measurement method, measuring the amount of light deflected by the particles in the exhaust gases. Due to its measurement principle it is mainly sensitive to particles [15]. Although it proved to be well applicable for PTI exhaust measurements, it has not been approved by the governments yet. Some other new measurement methods have been proposed, but without success [16, 17]. As an alternative researchers focused on updated versions of the opacimeter featuring an increased sensitivity. Generally it is possible to lower the detection limit by at least one order of magnitude with moderate means.

However opacimeters measure the combinational absorbing effect of all exhaust components within the green wavelength range, where the human eye has its maximum sensitivity. Originally this was by intention. It was the goal to measure an overall visual obstruction produced by the vehicle. Besides, for older vehicles, most of the effect could be attributed to the PM part. With the reduction of the particle emissions the attenuating effect of the brown NO_2 can surpass that of the particles. In such a case it might often be desirable to obtain additional information about the source of the measured signal in order to quickly identify the related defects in the exhaust system. Furthermore getting individual figures for PM and NO_X or NO_2 can be advantageous regarding the individual limitation of these two criteria pollutants. A one year study performed by the International Motor Vehicle Inspection Committee (CITA) in 2011 already investigated PTI test equipment for individual measurement of said components [13].

As shown in the following sections such extended measurement results can be achieved by an opacimeter enhanced with a multi-wavelength light source.

2 The Opacimeter

A standard opacimeter consists of a measurement chamber of defined length, a single-color, typically green light source on one side of the chamber and a light detector on the opposite side (see Fig. 2). As long as the measurement chamber contains clean air, the light emitted by the light source (e.g. a light emitting diode, LED) does not get attenuated and a nominal light intensity I_0 is measured on the detector (e.g. a photo diode). During the measurement the chamber is filled with the exhaust sample, which attenuates the light, resulting in a decreased light intensity

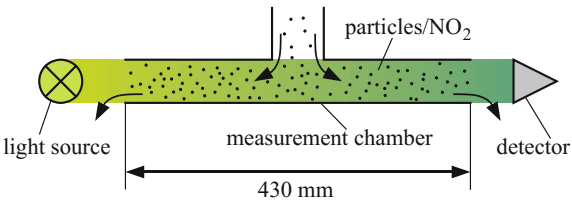

Fig. 2 Measurement principle of an opacimeter

I at the detector. By relating the two intensities I and I_0 to each other the opacity N can be calculated as

$$N = 1 - (I/I_0). \tag{1}$$

The opacity N is given in %. It depends on the length of the measurement chamber. Typically a length of 430 mm is used, but differing values are possible. Generally a length-independent measurement value is preferred. Therefore the so-called extinction coefficient k is typically determined along with or instead of the opacity. It is given in 1/m and can be calculated from I, I_0 and the effective measurement length L_{eff} using Lambert's Law [19]:

$$I/I_0 = \exp(-kL_{\text{eff}}) \tag{2}$$

In the literature this equation is also often called Lambert-Beer or Beer-Lambert law. However the name Lambert-Beer law designates a slightly different variation of (2), where the extinction coefficient is replaced by the product of the concentration c of the absorbing material and its extinction efficiency σ_{ext} [18]:

$$I/I_0 = \exp(-c\sigma_{\text{ext}}L_{\text{eff}}) \tag{3}$$

Accordingly one can determine the concentration of the absorbing material from the opacity measurement, if the extinction coefficient σ_{ext} is known and constant. The following section describes the physical background of said values and shows typical values for PM and NO_2.

3 Absorption of Particles and Gases

When light travels through a medium, energy is partly removed from the light beam by the obstacles (particles, gas molecules and atoms) in the medium. This results in an attenuation of the light beam. Such an effect is called extinction [19]. It is the combination of absorption, where energy is transferred from the incident beam to the obstacles, and scattering, where some parts of the light beam are deflected from the original path and thereby also removed from the incident beam. Mathematically this can be described in terms of the cross sections

$$\sigma_{ext} = \sigma_{abs} + \sigma_{sca}, \tag{4}$$

where σ_{abs} and σ_{sca} are the absorption and the scattering cross sections respectively [20]. The concept of a cross section is used to describe the ability of an obstacle to remove light from an incident beam in a simple way. It can be understood as the area shadowed from the incident beam. For the case of exhaust the main contributor to extinction is absorption. This is attributable to the strong absorbing effects of the primary components of the exhaust. Soot particles have a scattering share of only 10–30 % [21, 22]. Gases like NO_2 even have a negligible scattering effect [23]. This is the reason why, although physically incorrect, it has become customary to call k absorption coefficient rather than extinction coefficient.

The total extinction coefficient of a mixture of substances with differing extinction coefficients k_i can be determined by summation [24]. As in (3) k_i can be expressed by the products of the individual cross sections $\sigma_{ext,i}$ and the respective concentrations c_i. Accordingly the total extinction coefficient k can be calculated as

$$k = \sum_i k_i = \sum_i c_i \sigma_{ext,i}. \tag{5}$$

In principal the extinction cross section of the essential components in the exhaust of diesel engines, PM and NO_2, can be calculated with well-known formulas. For species very small compared to the incident wavelength, e.g. gas molecules, the shape of the object can be approximated as a sphere. In such a case the Rayleigh model can be used to calculate scattering, absorption and extinction effects. The Rayleigh model is valid, as long as the elements are smaller than approximately one tenth of the wavelength. For bigger elements, like accumulation mode exhaust particles [3], the shape must be taken into account. The behavior of spherical objects can be calculated using the Mie theory, which is applicable for any sphere diameter. Exact formulas also exist for some other well-defined shapes. For irregular objects like the fractal-like soot particles, one typically uses approximative models like the Rayleigh-Debye-Gans model for fractal aggregates (RDG-FA) [15].

For the purpose of this work it is important to understand the influence of the wavelength on the extinction behavior. Accordingly the extinction spectrum over a wide wavelength range is needed. The exact quantum-chemical calculation of such a spectrum is yet not possible [25]. Fortunately especially for gases there exists elaborate measurement data of the absorption behavior. For diesel soot particles there exists extinction data, too, though not to the same amount.

3.1 Absorption of NO_2

As said before the scattering effect of gases like NO_2 is negligible. Its extinction cross section is therefore almost identical to the absorption cross section, which is shown in Fig. 3 for the wavelength range from 250 to 800 nm, given in

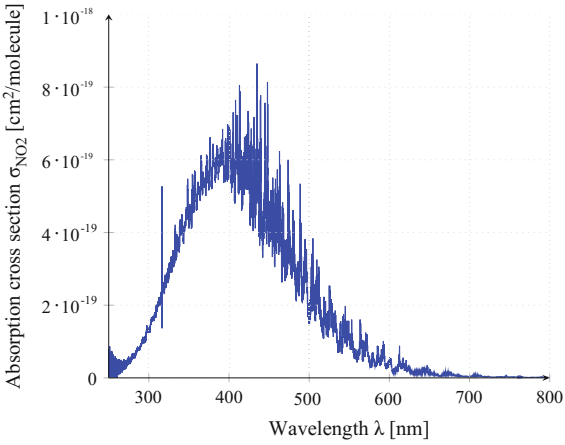

Fig. 3 Absorption cross section of NO_2

cm^2/molecule [26]. It has been measured at a pressure of 1000 mbar and a temperature of 293 K.

Generally the uncertainty is in the order of a few percent. Near 250 nm the uncertainty increases, as oscillations occur that are physically implausible. The peak around 316 nm seems to be an artefact, too. Both phenomena are not of importance for the actual work. The high oscillations around the peak at approximately 400 nm however are factious. Thus it is crucial to utilize data with high wavelength resolution in this area in order to achieve proper results. Temperature and pressure also have a notable influence on the absorption behavior. Those influences can be compensated using empirical models [25, 27].

3.2 Extinction of Soot Particles

The extinction behavior of particles is shown in Fig. 4 based on the example of a Volkswagen turbo diesel engine (TDI Type 1Z, 1.9 l, 66 kW). It is given for the wavelength range from 230 to 1000 nm in m^2/g [28, 29]. In contrast to NO_2 the spectrum is rather smooth. According to their black color the soot particles absorb light quite equally in the whole visible wavelength range. The measurement uncertainty of the given data is in the order of 5 %. It has however not been measured directly at the tailpipe. The particles had already grown to a median mobility diameter (MMD) of 250–300 nm due to coagulation, which is approximately three times bigger than the MMD of tailpipe particles. The actual effect of particle size on the extinction is rather small. The bigger particles will result in a slightly stronger extinction. This is due to an increased scattering cross section, the absorption cross section of fractal-like soot aggregates with constant volume is independent of the particle size [30]. Simulations performed with typical particle

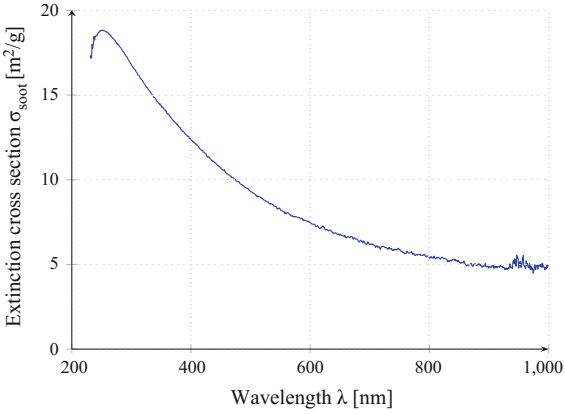

Fig. 4 Extinction cross section of diesel soot

size distributions of diesel exhaust [3, 31] predict deviations in the order of a few percent.

The absorption spectrum of NO_2 and the extinction spectrum of soot are very different, as obvious from Figs. 3 and 4. Accordingly their corresponding extinction effects differ substantially for e.g. red, green and blue light. This is used in the multi-wavelength approach presented in the following section.

4 The Multi-wavelength Approach

An examination of smoke samples using light at multiple wavelengths has already been performed in the past. Aspey and Brazier for example have investigated the particle mass fraction and mean particle size in exhaust [32]. Sharma et al. performed optical characterizations of aerosols using a multi-wavelength photoacoustic-nephelometer spectrometer [33]. Haisch and Niessner presented a photoacoustic analyzer for the simultaneous quantification of soot and NO_2 in engine exhaust [34]. In this work a similar approach is adopted for an opacimter: Using a multi-wavelength light source the individual contributions of soot and NO_2 to the opacity are determined and the respective concentration values are derived.

For this purpose the extended opacimeter performs multiple consecutive measurements of the smoke sample using different wavelengths. Any wavelengths for which the extinction differs sufficiently could be used. Standard opacimeters are equipped with a green light source. To support normal opacity measurements the green light source can be retained and a red and blue light source added. The according measurement setup is shown in Fig. 5. In each measurement *i*, where one of the light sources is enabled at a time, the equation

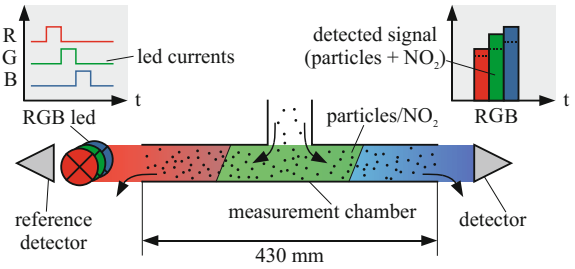

Fig. 5 Three wavelength measurement setup

$$k_i = k_{NO_2}(\lambda_i) + k_{soot}(\lambda_i) + k_{other}(\lambda_i) \tag{6}$$

holds. Herein λ_i is the wavelength of each light source, k_{NO_2}, k_{soot}, k_{other} and k_i are the individual extinction coefficients of NO_2, soot particles and other components and the total extinction coefficient at the given wavelength λ_i respectively. The equation can be rewritten as in (5) using the product of the concentrations c_x and the extinction cross sections σ_x, leading to

$$k_i = c_{NO_2}\sigma_{NO_2}(\lambda_i) + c_{soot}\sigma_{soot}(\lambda_i) + c_{other}\sigma_{other}(\lambda_i). \tag{7}$$

When performing three measurements of the same sample (i.e. the concentrations c_x remain constant during the whole measurement time) an equation system with three equations and also three unknowns is obtained. This of course requires knowledge of all extinction cross sections. In such a case, the matrix equation

$$\begin{pmatrix} k_1 \\ k_2 \\ k_3 \end{pmatrix} = \begin{pmatrix} \sigma_{NO_2}(\lambda_1) & \sigma_{soot}(\lambda_1) & \sigma_{other}(\lambda_1) \\ \sigma_{NO_2}(\lambda_2) & \sigma_{soot}(\lambda_2) & \sigma_{other}(\lambda_2) \\ \sigma_{NO_2}(\lambda_3) & \sigma_{soot}(\lambda_3) & \sigma_{other}(\lambda_3) \end{pmatrix} \begin{pmatrix} c_{NO_2} \\ c_{soot} \\ c_{other} \end{pmatrix} \tag{8}$$

can ideally be solved by simple matrix inversion.

For σ_{other} a representative absorber besides soot and NO_2 should be chosen. In practice the composition of the exhaust samples might vary to such a degree that the selection of a single representative absorber is not possible. In that case it can be omitted, leading to an over-determined system. Such a system can be solved using a least-squares algorithm to calculate the best fit for the remaining two components.

5 Technical Realization

5.1 Physical Setup

The multi-wavelength opacimeter is built from the basis of a highly sensitive single-pass opacimeter, as depicted in Fig. 5. In order to achieve a sufficiently high

sensitivity in the order of $\Delta k = 0.001\ m^{-1}$ the optical path length and hence the measurement chamber should not be too small. We used a cylindrical cell with a diameter of 2.4 cm and a length of 400 mm, where the axis of the cylinder coincides with the optical axis of the system. The inlet for the smoke sample is placed in the middle of the chamber. The exhaust is filled into the chamber by the dynamic pressure in the exhaust pipe. It leaves the chamber through the in-/outlet for the light beam.

A flow of sheath air transports the exhaust sample to the smoke outlet. The sheath air flow is produced from ambient air by filtration using a high-efficiency particulate air (HEPA) filter. On the one hand the sheath air protects the optical setup from contamination, on the other hand it defines the length of the optical path. As the optical path length directly influences the measurement value, it is crucial to keep the optical path length constant. Therefore the sheath air flow needs proper fluid dynamical considerations.

In Fig. 6 a multiphysical complex fluid dynamic simulation result is shown. The ratio of exhaust gas entering through the middle section of the measurement cell to the air flow rate through the sheath air channels defines the optical path. In order to quantify a representative exhaust gas sample within the measurement cell, the distribution of the analytes should be homogeneous, independently of the dynamic pressure in the exhaust pipe. A proper fluid dynamic design and hence an iterative optimization approach by means of complex fluid dynamics is a necessary prerequisite to obtain meaningful measurement results.

For the light source it is advantageous to use a realization that combines the three colors into a single housing. That ensures comparable optical behavior of the

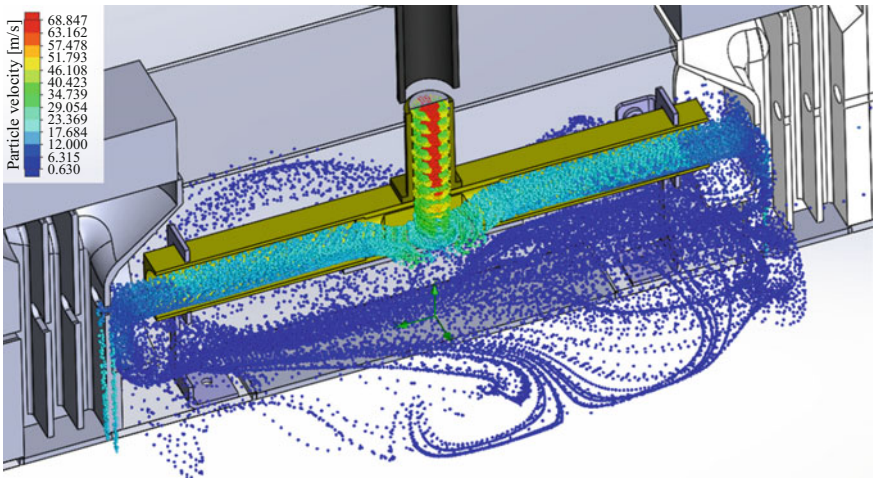

Fig. 6 Multiphysical complex fluid dynamic simulation of the measurement cell. The points represent particle ensembles with particle velocities scaled by the color. A homogeneous velocity distribution within the optical path guarantees representative samples of the exhaust gas portion to be quantified

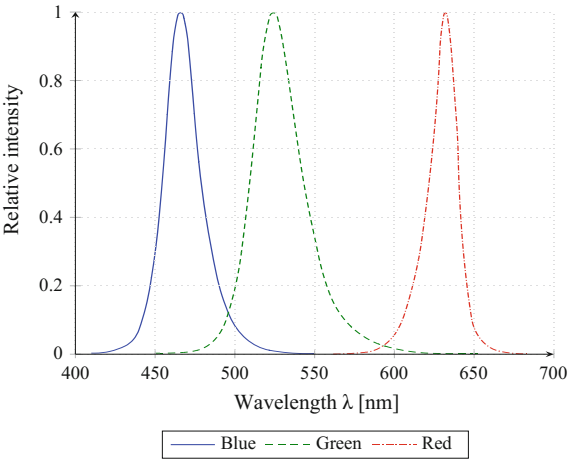

Fig. 7 Relative intensities of the used multi-color LED

different colors due to their proximity. To increase signal-to-noise ratio and reduce the challenges for amplification on the receiver side, the light source should have a high intensity. This is achievable with a commercially available high power LED, like for instance the OSRAM LRTB. Its three dominant wavelengths are at 632, 523 and 455 nm for the red, the green and the blue color respectively (see Fig. 7).

The incident light is collimated by means of an aspherical lens (optical parameters: $d = 18$ mm, $f = 15$ mm, $bfl = 11.10$ mm, $Md = 6$ mm), resulting in a beam divergence of typically less than 8°. If needed the beam divergence can be adapted by changing the distance between the lens and the LED.

On the receiver side an optical detector converts the incident light into the electrical domain. For this purpose a PIN photodiode with a large optical area of 7 mm^2 is used. A collimating lens, identical to the one on the transmitter side, is placed in front of the photodiode, to maximize the incident intensity and overcome losses due to misalignments produced by vibrations and shocks. As the measurement signal is directly proportional to the source light intensity, a stable source is of high importance. Nevertheless if fluctuations occur they can be compensated via a reference photodiode, measuring the current source intensity.

5.2 Electronic Measurement Circuitry

The optical measurement principle is based on the attenuation of light in the measurement chamber. An absence of particles or light absorbent gases corresponds to a full scale reading at the optical receiver. As a consequence, any gain or offset error/drift of the optical measurement directly and significantly influences the reading.

Numerical post-processing involves the subtraction of the actual optical output level from the reference output level and scaling this difference by the appropriate sensitivity coefficient. Both resolution and accuracy of the optical detector, its associated transconductance amplifier and the analog-to-digital converter (ADC) have to be adequately high, such as to compensate for the loss of significant digits in the following calculations.

The opacity as a ratio of I/I_0 is a dimensionless quantity, which naturally suggests a fully ratiometric measurement setup. Second order effects would still have an influence, such as gain and offset errors of the amplifiers or nonlinearities of the ADC. However, these can be kept well within allowable limits by careful circuit design.

Figure 8 shows an idealistic approach of a fully ratiometric light absorption measurement setup. The light emitted by the LED at the transmitter side is divided into two paths: The first illuminates the measurement cell containing the analyte, the second serves as a reference. An optical multiplexer at the receiver side alternately lets one of the two signals pass to the optical receiver diode. Errors related to the electronic instrumentation would largely cancel out, since the measurement and reference phase use the same optical detector and signal conditioning circuitry. Some nonlinearity would still remain, in the first instance related to the ADC.

Such an approach is not feasible for some reasons: the mechanical construction including the optical multiplexer is costly and moderately reliable, and both the optical transmitter and the optical receiver have a linear relationship between optical power and electrical current, not voltage. In contrast, the electrical signal conditioning is based on a reference voltage. It is the reference for the ADC at the receiver side and the digital-to-analog converter (DAC) for adjusting the LED

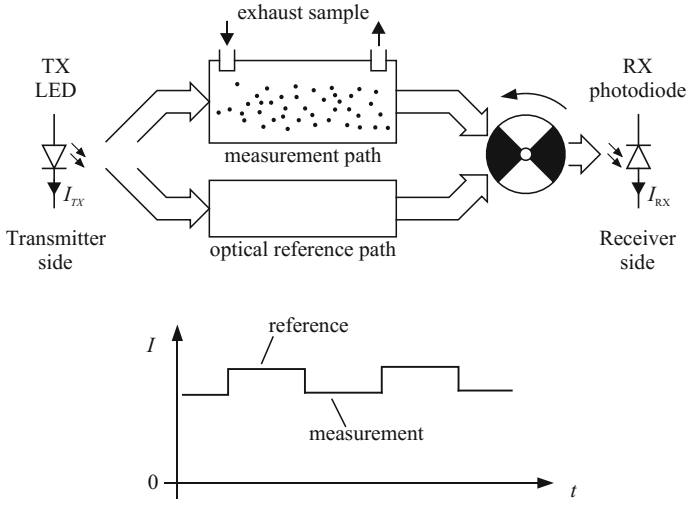

Fig. 8 Ideal approach of a fully ratiometric light absorption measurement

power at the transmitter side. As a consequence, at least two precision resistors are needed: one is part of the voltage controlled current source for the transmitter LED, another one is part of the transimpedance amplifier, converting the current output of the photodiode into a voltage output for the ADC.

Figure 9 represents the actual setup. The electronic instrumentation relies on the ratiometric principle to a great extent. A set of two identical optical receivers replaces the optical chopper of Fig. 8, each one including its dedicated transimpedance converter. A total of three precision resistors ($R_{\mathrm{REF,TX}}$, $R_{\mathrm{REF,RX,1}}$ and $R_{\mathrm{REF,RX,2}}$) are required, which is acceptable because these parts are available with excellent specifications for tolerance, temperature coefficient and long-term stability.

The optical output power of the LED correlates with its forward current. It is adjusted by the setting of the DAC, its reference voltage and the transconductance of the voltage controlled current source. A digital control loop, implemented in the firmware of the microcontroller, uses the output voltage $V_{\mathrm{RX,2}}$ of the optical reference path to set the LED current I_{TX} and keep it at the desired set level.

At the receiver side there are two photodiodes, each with its dedicated transimpedance amplifier for the current-to-voltage conversion. A critical part for the overall performance of the measurement setup is the matching of the optical receivers and their interface electronics. The photodiodes operate in current (short circuit) mode. Their light-to-current transfer ratio is therefore highly linear over several decades of intensity. Thermal influences are low and further reduced by keeping both photodiodes at the same temperature.

The influence of dark current and bias currents at the receiver side are compensated by a reference measurement with the transmitter LED turned off. Minor deviations are canceled out by digital post processing; abnormally high deviations indicate a fault situation and are handled by self-diagnostic functions.

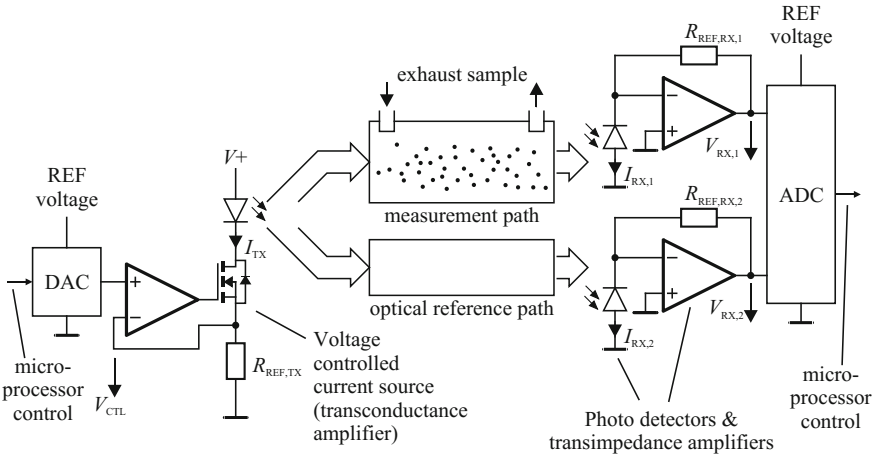

Fig. 9 Actual measurement setup

5.3 Mathematical Model

The measurement setup provides three extinction coefficients, each for one of the three used wavelengths λ_i. Equation (8) provides the equation system for determining the concentrations of three absorbing species from such a measurement. As mentioned above there is generally no exact solution for this equation system. Furthermore the third typical absorber in addition to soot and NO_2 can often not easily be identified. We therefore use the reduced equation system

$$\begin{pmatrix} k_1 \\ k_2 \\ k_3 \end{pmatrix} = \begin{pmatrix} \sigma_{NO_2}(\lambda_1) & \sigma_{soot}(\lambda_1) \\ \sigma_{NO_2}(\lambda_2) & \sigma_{soot}(\lambda_2) \\ \sigma_{NO_2}(\lambda_3) & \sigma_{soot}(\lambda_3) \end{pmatrix} \begin{pmatrix} c_{NO_2} \\ c_{soot} \end{pmatrix}, \tag{9}$$

which focusses on the two criteria pollutants particles and NO_2. In the discussion section we will show that this generally delivers good results for diesel engine exhaust.

The concentrations can be determined from (9) by inversion. This can be most easily achieved by multiplication with the pseudo inverse

$$A^+ = (A^T A)^{-1} A^T, \tag{10}$$

where A denotes the cross section matrix and A^T its transpose. It will yield the best fit for the solution in a least squares sense.

The cross section values $\sigma_x(\lambda_i)$ for NO_2 and soot can be taken from Figs. 3 and 4 respectively, as long as monochromatic light sources are used. The graphs however use different units for the cross section values. So a conversion of one of the cross sections to the unit of the other one is needed. We chose to use the unit m^2/g and converted the cross section for NO_2 as follows:

$$\sigma_{NO_2}\left[\frac{m^2}{g}\right] = \frac{1}{10^4}\sigma_{NO_2}\left[\frac{cm^2}{molecule}\right]\frac{N_A}{M_{NO_2}}\left[\frac{molecules/mol}{g/mol}\right] \tag{11}$$

Herein $M_{NO_2} = 46.005$ g/mol is the molar mass of NO_2 and $N_A = 6.022\ 10^{23}$ molecules/mol is the Avogadro constant.

Since we use a LED as a light source, the single colors are clearly not monochromatic. In this case the corresponding nominal intensities I_0 at the wavelengths λ_i have to be replaced by continuous nominal intensity spectra $I_0(\lambda)$ from Fig. 7, where at each wavelength λ (2) holds:

$$I(\lambda) = I_0(\lambda)\exp(-kL_{eff}) \tag{12}$$

On the detector the single intensities $I(\lambda)$ are integrated with respect to the spectral efficiency $\gamma(\lambda)$ of the detector:

$$I = \int \gamma(\lambda) I(\lambda) \mathrm{d}\lambda = \int \gamma(\lambda) I_0(\lambda) \exp(-kL_{\mathrm{eff}}) \mathrm{d}\lambda \tag{13}$$

The total nominal light intensity I_0 can be calculated accordingly. By relating I and I_0 a mean extinction coefficient $\bar{k}(\lambda_i)$ can be determined, as before, for each color λ_i:

$$\exp(-\bar{k}(\lambda_i) L_{\mathrm{eff}}) = \frac{\int \gamma(\lambda) I_0(\lambda) \exp(-k(\lambda) L_{\mathrm{eff}}) \mathrm{d}\lambda}{\int \gamma(\lambda) I_0(\lambda) \mathrm{d}\lambda} \tag{14}$$

In order to set up the equation system, the extinction coefficient is again replaced by the product of cross section and concentration, now denoted as $\overline{\sigma_x}(\lambda_i)$ and $\hat{c}$ respectively. However in the case of a polychromatic light source the strict proportionality does not hold for the mean values. This is obvious from the following equation:

$$\exp(-\hat{c}\overline{\sigma_x}(\lambda_i) L_{\mathrm{eff}}) = \frac{\int \gamma(\lambda) I_0(\lambda) \exp(-c\sigma_x(\lambda) L_{\mathrm{eff}}) \mathrm{d}\lambda}{\int \gamma(\lambda) I_0(\lambda) \mathrm{d}\lambda} \tag{15}$$

Despite the limited proportionality the model in (9) provides a good approximation to the real behavior, as shown by the simulations in the following discussion section.

6 Results and Discussion

The multi-wavelength approach has been evaluated using simulations and basic measurements. The results are presented and discussed in the following sections.

6.1 Sensitivity Measurements

Our first measurements have been performed with a new, highly sensitive opacimeter, to ensure that reliable measurements of the extinction produced by NO_2 are possible even at low concentrations. The opacimeter was equipped with a single color light source (green light with Gaussian intensity spectrum, $\mu = 560$ nm, $\sigma = 8$ nm). The resolution was 0.001 m^{-1}. The results are shown in Fig. 10.

Conforming to theory the measured extinction value is linearly related to the NO_2 concentration. The smallest resolvable NO_2 concentration is in the order of 10 ppm. Compared to simulations the measured extinction coefficient is a bit lower. The simulated value at 1000 ppm was approximately 0.2 m^{-1}, whereas the

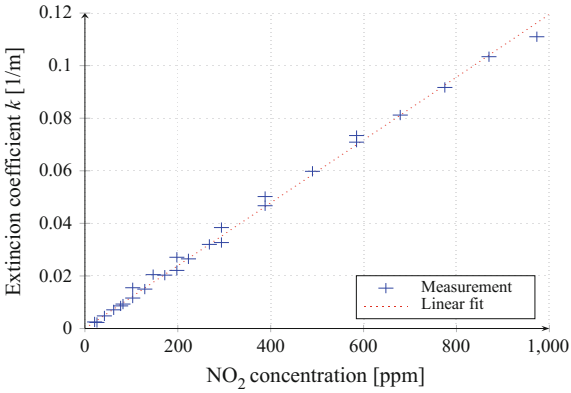

Fig. 10 NO_2 measurements with a new opacimeter

measured value is 0.12 m^{-1}. The deviations can probably be attributed to different ambient conditions (pressure and temperature).

6.2 Mathematical Simulations

The simulations have been performed in MATLAB using the model from (9) with the cross section spectra presented in Figs. 3 and 4. Combinations of NO_2 at concentrations from 100 to 1000 ppm and soot particles at concentrations from 1 to 1000 mg/m^3 have been tested. The results for the estimation of the NO_2 concentration from the simulated values are depicted in Fig. 11 for the noise-free case in the form of the relative deviation from the actual concentration.

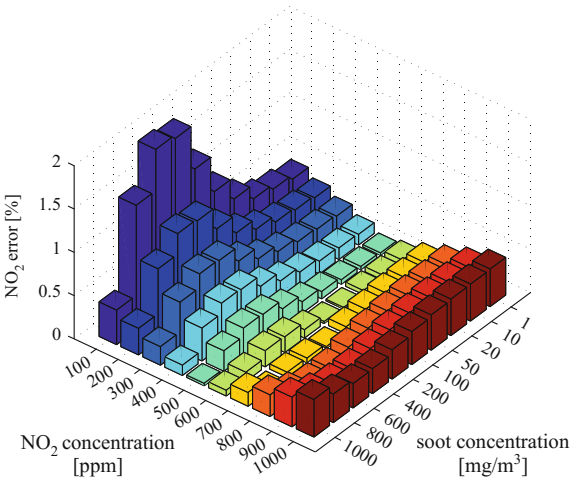

Fig. 11 Error in calculated NO_2 concentrations (simulation without noise)

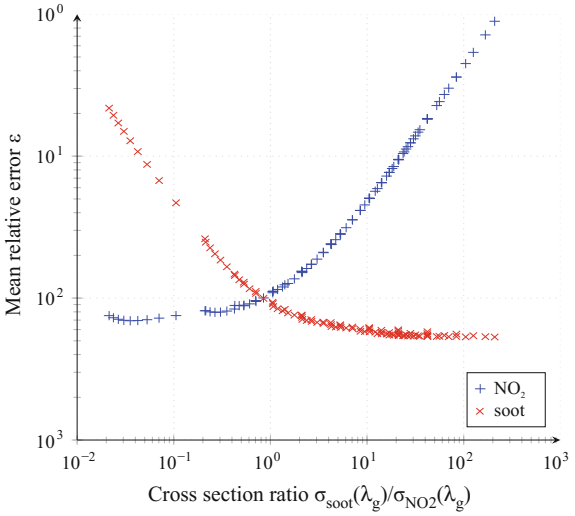

Fig. 12 Mean error in calculated NO_2 and soot concentrations (simulation with 1 % of noise)

For most combinations the error is below 1 %. Only if the contribution of one component is very low, e.g. 100 ppm of NO_2, the error can increase to almost 2 %. The reason for this error in the noise-free system is the limited proportionality due to polychromatic light. Consequently the systematic error can be reduced, when light sources with a narrow wavelength spectrum or quasi-monochromatic light sources like lasers are used.

If noise is applied the errors generally rise to a few percent. The relative error for 1 % of noise is depicted in Fig. 12. Larger errors between 10 % to 40 % for the NO_2 concentrations are only found when the contribution of soot is at least twenty times higher than that of NO_2. Solely if the share of NO_2 is smaller than 1/100 and hence negligible the mean error rises above 40 %. For the particle concentration small errors below 2.5 % can be achieved for all combinations where $c_{soot} \geq 10$ mg/m^3.

6.3 Discussion

Both preliminary measurements and simulations indicate a good applicability of the described multi-wavelength approach. Further measurements are planned for the future to investigate the performance on both laboratory mixtures of particles and NO_2 and real-world exhaust samples.

As our measurements have shown so far, it is advantageous to perform calibration measurements to acquire the cross section matrix for concentration measurements. The simulations can be a great tool for evaluating the method in theory but may result in somewhat deviating numbers.

With a calibration based on practical measurements we except good results for the determination of the concentrations of NO_2 and particles, as long as they are the

primary contributors to the extinction. Other strong absorbers present in the exhaust sample might lead to deteriorated results. For diesel exhaust this is a rare case. Known examples of additional absorbers are white and blue smoke. White smoke, produced by condensed water, can be eliminated by proper conditioning of the engine prior to the PTI and by heated sample lines. By keeping the exhaust temperature above the due point of exhaust gases, which is in the area of 45–55 °C [14], water is hindered from condensing. When using a temperature above 100 °C already condensed droplets can be evaporated again. Blue smoke is typically related to an engine defect. It can occur for instance, if oil leaks into the cylinder [35–38]. If required, such hydrocarbon emissions can be eliminated by integration of an oxidation catalyst ("catalytic stripper") into the heated sample line [39]. Hence, when implementing such measures, an overall good applicability to real engine emissions can be assumed.

For the real-world exhaust samples comparison measurements with dedicated NO_2 sensors are planned to gain insights into the quality of the measurement results. Although such dedicated devices will of course yield more accurate results [40], the proposed method can provide at least valuable qualitative results without the need for extra measurement equipment. Furthermore little or no additional conditioning of the exhaust sample is needed in comparison to a standard opacimeter. Finally the main functionality of the opacimeter, i.e. measuring the exhaust opacity, is not degraded in any way.

7 Conclusion

Emission regulation covering the whole lifetime of vehicles is a key for a clean and healthy environment. Two of the main pollutants of combustion engines, namely soot and nitrous oxides, depend strongly on the state of health of the combustion engine as well as of the exhaust aftertreatment system. Within this chapter a novel method for the simultaneous determination of NO_2 and soot in the exhaust of diesel engines with emphasis on periodical technical inspection (PTI) was elaborated in detail. It is based on a spectroscopic multi-wavelength light extinction measurement in a setup similar to an opacimeter with high sensitivity. Preliminary experimental results have proven its ability to reliably detect small concentrations of NO_2 with a limit of detection (LOD) as low as 10 ppm. The experimental research with the focus on the simultaneous determination of the second pollutant soot is ongoing. The overall results are promising and indicate the potential to gain further information on the pollutants contained in exhaust without the need for an additional dedicated sensor in PTI applications.